ARTICLE NO. 79-0207R

Downstream Mixing Gasdynamic Lasers—A Numerical Solution

K. N. Parthasarathy,* J. D. Anderson Jr.,† and E. Jones‡
University of Maryland, College Park, Md.

Time-dependent finite-difference solutions of the two-dimensional Navier-Stokes equations, fully coupled with the appropriate finite-rate vibrational kinetic equations, are obtained for a CO_2-N_2 downstream-mixing gasdynamic laser (GDL). Low Reynolds numbers, hence laminar mixing flows, are studied. Optimum results for laser gain are obtained with no velocity discontinuity between the mixing streams, and with no catalyst (H_2O) present in the mixture. Local small-signal gains as high as 13.5/m are calculated for a 4000 K N_2 reservoir temperature. Although the present analysis deals only with small-signal gain (no power extraction), the results underscore the potential superiority of downstream-mixing GDL's over conventional designs.

I. Introduction

BASOV and Oraevskii[1] suggested that population inversions in molecuar systems could be created by rapid heating or cooling of the system. Hurle and Hertzberg[2] suggested that such cooling and population inversions could be obtained in the rapid, nonequilibrium expansion of an initially hot gas through a supersonic nozzle. These ideas were utilized in the construction and successful operation of a high-power continuous wave gasdynamic laser at the Avco Everett Research Laboratory in 1966.[3] This was the first gasdynamic laser of its kind, and it utilized a mixture of CO_2-N_2-H_2O. In such a conventional gasdynamic laser, a mixture of hot high-pressure gases is expanded very rapidly through a supersonic nozzle. During this rapid expansion, the gas becomes a lasing medium, i.e., a population inversion is created in the gas. If mirrors are placed on both sides of the test section downstream of the nozzle exit, then a beam of laser energy is extracted perpendicular to the flow from this supersonic laser gas. The supersonic stream then enters a diffuser and generally exhausts to the atmosphere.

In the conventional CO_2-N_2-H_2O gasdynamic laser (GDL) just described, although the lasing medium is CO_2, the primary source of energy for pumping the CO_2 comes from vibrationally excited N_2. In this conventional GDL setup, the CO_2 and H_2O act as contaminants of the N_2. As a result, the CO_2-N_2-H_2O mixture relaxes faster than pure N_2, giving lower vibrational temperatures and hence lower available laser power. Furthermore, the higher the reservoir temperature, the more vibrational energy is present in the gas, and subsequently more laser power can be obtained. But in conventional GDL's there is an upper limit of approximately 2300 K on this temperature. Above this, the CO_2 begins to dissociate, and laser performance begins to deteriorate. By comparison, the dissociation temperature of N_2 is above 4000 K.

In contrast, in a downstream-mixing gasdynamic laser, pure N_2 is expanded through a supersonic nozzle and mixed with CO_2 and H_2O downstream of the nozzle exit. The major advantages are 1) reservoir temperatures of N_2 can exceed 4000 K, and 2) more efficient freezing of the N_2 vibrational energy is obtained.

From the preceding discussion, downstream-mixing GDL's appear to have tremendous potential. In fact, a simple calculation for N_2 with $T_0 = 4000$ K and $p_0 = 108$ atm expanding through a nozzle with an area ratio of 175 and a throat height of 0.1 mm, and instantaneously mixing with CO_2 and H_2O downstream of the nozzle exit, yields a maximum available energy of over 300 KJ/lb.[4] This is more than an order-of-magnitude larger than the best figure for conventional GDL's. This quantum jump in energy is the result of the assumption of instantaneous mixing. Obviously, this does not occur in real life. In the actual mixing region, it takes a finite amount of time for the molecular collisions to occur before the N_2 can pump the CO_2 molecules. Further, the vibrational deactivation will decrease the available power. Also, the rise in static temperature due to total temperature recovery in the mixing region will degrade the laser power output. The question is: Do the above effects associated with the real aspects of mixing completely negate the whole concept of the downstream-mixing gasdynamic laser? If not, to what extent can the laser performance be achieved? The present work provides some answers to these questions.

The concept of the downstream-mixing gasdynamic laser has been studied since 1970 by various investigators.[5-8] In particular, Taran et al.[6] observed that mixing of the streams downstream of the nozzle exit resulted in low laser gains because a substantial portion of the total temperature is recovered in the mixing zone. They found that improvement in laser gain could be obtained by mixing just downstream of the nozzle throat rather than at the exit. Croshko et al.[7] have also used mixing in the throat region. However, such mixing inside the nozzle is a compromise of the downstream-mixing concept as originally described. Recently, Cassady et al.[8] have shown the viability of the downstream-mixing concept using an array of screen nozzles. They reported gains of 1.5/m and 30 KJ/lb of energy in the laser cavity.

The present work makes two main contributions to the state-of-the-art; the first is computational, and the second pertains to the laser results themselves. In particular:

1) This is the first solution of the downstream mixing gasdynamic laser flows utilizing the complete two-dimensional Navier-Stokes equations, fully coupled with the finite-rate vibrational rate equations. Therefore, this analysis allows the direct calculation of pressure gradients as a natural part of the solution, in contrast to previous boundary-layer solutions which usually assume constant pressure everywhere. Moreover, it provides the future capability of dealing with separated and reverse flows in the base region of the nozzles.

Presented as Paper 79-0207 at the 17th Aerospace Sciences Meeting, New Orleans, La., Jan. 15-17, 1979; submitted Jan. 22, 1979; revision received May 7, 1979.

Index categories: Lasers; Viscous Nonboundary-Layer Flows; Computational Methods.

*Graduate Research Assistant, Dept. of Aerospace Engineering. Student Member AIAA.

†Professor and Chairman, Dept. of Aerospace Engineering. Associate Fellow AIAA.

‡Associate Professor, Dept. of Aerospace Engineering. Member AIAA.

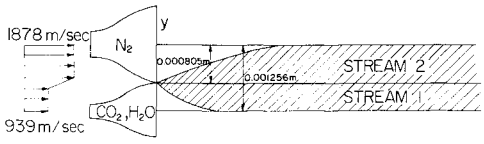

NOZZLE CONFIGURATION

	STREAM 1	STREAM 2
P n/m²	656	656
T °K	300	300
ρ Kg/m³	1.094×10^{-2}	7.36×10^{-3}
ρ_{CO_2} Kg/m³	1.051×10^{-2}	–
ρ_{H_2O} Kg/m³	4.28×10^{-4}	–
MACH NO.	5.32	3.33
T_{VIB} °K	300	2000

INITIAL CONDITIONS

Fig. 1 Schematic of the downstream-mixing GDL and initial conditions.

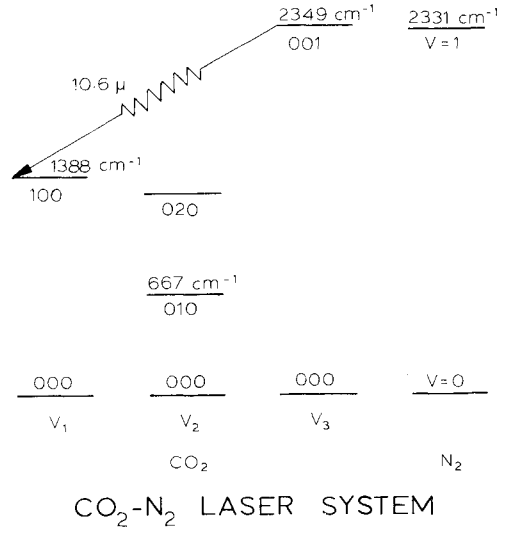

Fig. 2 Energy level diagram.

2) The laser results are themselves new. After a reasonable set of numerical experiments examining the influence of various parameters at low Reynolds number, hence encouraging laminar flow, it was found that:

a) The higher laser gain occurred with no velocity discontinuity between the two streams; the most efficient mixing process was essentially one of mass diffusion.

b) Optimum gain occurred with no H_2O present in the mixture. It should be noted here that though H_2O is detrimental to *gain*, it is vital to power *extraction*. Hence, downstream mixing GDL's do need H_2O to enhance power extraction. Also, refer to discussion of effect of H_2O content on small-signal gain in Sec. IV of this paper.

c) In the calculations for the 4000 K reservoir temperature, local small-signal gains as high as 13.50/m and average small-signal gains as high as 11.7/m were obtained. These appear to be the highest values noted in the literature for realistic viscous mixing flows. Consequently, the concept of low Reynolds number, laminar, downstream-mixing gasdynamic lasers may be worth serious future investigation.

II. Physical Problem and Analysis

Figure 1 illustrates the physical setup of the downstream-mixing GDL. Here, a supersonic stream of N_2 is mixed with a supersonic stream of CO_2 and H_2O. The conditions shown in Fig. 1 are typical of the cases studied. The nozzles are sized to give an N_2, CO_2, H_2O mole ratio of 78:20:2 in the cavity. The nozzles are very small and the pressures are low, leading to Reynolds numbers on the order of 10^3 (based on the distance between centerlines). Hence, the flow is assumed to be laminar. Uniform but different flow properties are assumed at the exit of each nozzle exhausting into the laser cavity.

For the low Reynolds numbers involved, thick boundary layers will be formed within the nozzles. The effect of such boundary layers is presently being studied, but will not be discussed here. Instead, the purpose of the present results is to isolate and study the fluid dynamics of mixing between two initially uniform, parallel streams. The flowfield properties are calculated as functions of x (in the flow direction) and y (normal to the flow direction) in the laser cavity by solving the unsteady, laminar, Navier-Stokes equations along with the vibrational rate equations.

Vibrational Model

In a CO_2-N_2-H_2O gasdynamic laser, as mentioned earlier, CO_2 is the lasing molecule and the N_2 molecule transfers its energy to pump up the CO_2 molecule. CO_2 is a linear, triatomic molecule with the three modes of vibration—a symmetric stretch mode with fundamental freqency ν_1, a doubly degenerate bending mode with frequency ν_2, and an asymmetric stretch mode with frequency ν_3. N_2, which is a diatomic molecule, has only one mode of vibration with a fundamental frequency of ν. The energy level diagram for the CO_2-N_2 system is shown in Fig. 2. The laser transition between 001 and the 100 levels of CO_2 is also indicated in the figure. Taylor and Bitterman[9] have cataloged the various vibrational energy processes that occur in the CO_2-N_2-H_2O system. The detailed energy transfer processes can be written as follows:

T-V Processes

$$CO_2^*(\nu_2) + M \rightleftharpoons CO_2 + M + 667 \text{ cm}^{-1} \quad (1)$$

$$N_2^* + M \rightleftharpoons N_2 + M + 2331 \text{ cm}^{-1} \quad (2)$$

V-V Processes (Intermolecular)

$$CO_2^*(\nu_3) + N_2 \rightleftharpoons CO_2 + N_2^* + 18 \text{ cm}^{-1} \quad (3)$$

V-V Processes (Intramolecular)

$$CO_2^*(\nu_3) + M \rightleftharpoons CO_2^{**}(\nu_2) + M + 416 \text{ cm}^{-1} \quad (4)$$

$$CO_2^*(\nu_1) + M \rightleftharpoons CO_2^{**}(\nu_2) + M + 102 \text{ cm}^{-1} \quad (5)$$

In the foregoing equations, M stands for a collision partner that can be CO_2, N_2, or H_2O. The asterisks indicate the vibrational level in a given mode. Here are some pertinent observations of the CO_2-N_2 system:

1) The 001 level of CO_2 and $v=1$ level of N_2 have almost the same energy, separated by only 18 cm^{-1}. This implies that the pumping reaction given by Eq. (3) is near resonant and extremely fast.

2) The population of the upper laser level (001) is dependent on the population of $N_2 = v = 1$ level through the pumping reaction, Eq. (3). In addition, it also depends on the rate of reaction (4) and on the rate of laser power extraction, which tends to deplete the 001 level.

3) The 100 and 020 levels are relatively close. The Fermi resonance that exists between these two levels makes reaction (5) very fast.

4) The population of the lower laser level (100) is dependent on the rate of laser power extraction, which tends to fill the level, and on population of the 020 level via reaction (5).

These observations lead to a simplified model of the vibrational kinetic processes as described below.

Munjee's Model[10]

Let e_1, e_2, e_3, and e_4 be the vibrational energies for the ν_1, ν_2, and ν_3 modes of CO_2, and for N_2, respectively. Also, let T_1, T_2, T_3, and T_4 be the corresponding vibrational temperatures, all different from each other and from the static temperature T of the gas. In this model, it is assumed that the strong Fermi resonance between 100 and 020 levels leads to a coupling between the ν_1 and ν_2 modes and, hence, to the existence of a local equilibrium between these two modes. As a result, the energies e_1 and e_2 are combined together to give $e_{12} = e_1 + 2e_2$. Also, $T_{12} = T_1 = T_2$. The time rate of net energy transfer into or out of these modes are given by de_{12}/dt, de_3/dt, and de_4/dt. The expressions for these time derivatives, denoted by $\dot{w}_{12}$, $\dot{w}_3$, and $\dot{w}_4$, are

$$\dot{w}_{12} = 2[Z_{CN} P(\overset{10}{C}2,N) + Z_{CH} P(\overset{10}{C}2,H) + Z_{CC} P(\overset{10}{C}2,C)] \times [\exp(-\theta_2/T)\theta_2 R_{CO_2} - e_2(1-\exp(-\theta_2/T))] + 6\theta_2 R_{CO_2} \cdot \left\{[Z_{CN} Q_N(\overset{03}{C}2,\underset{10}{C}3) + Z_{CH} Q_H(\overset{03}{C}2,\underset{10}{C}3) + Z_{CC} Q_C(\overset{03}{C}2,\underset{10}{C}3)] \cdot \left[\frac{e_3}{\theta_3 R_{CO_2}}\left(\frac{e_2}{\theta_2 R_{CO_2}} + 1\right)^3 - \left(\frac{e_2}{\theta_2 R_{CO_2}}\right)^3 \times \left(\frac{e_3}{\theta_3 R_{CO_2}} + 1\right)\exp\left(\frac{3\theta_2 - \theta_3}{T}\right)\right]\right\} \quad (6)$$

$$\dot{w}_3 = [Z_{CC} Q_C(\overset{03}{C}2,\underset{10}{C}3) + Z_{CN} Q_N(\overset{03}{C}2,\underset{10}{C}3) + Z_{CH} Q_H(\overset{03}{C}2,\underset{10}{C}3)] \times \left[\exp\left(\frac{3\theta_2 - \theta_3}{T}\right)\left(\frac{e_2}{\theta_2 R_{CO_2}}\right)^3 (e_3 + \theta_3 R_{CO_2}) - e_3\left(\frac{e_2}{\theta_2 R_{CO_2}} + 1\right)^3\right] + Z_{CN} Q(\overset{01}{N},\underset{10}{C}3)\left[\exp\left(\frac{\theta_4 - \theta_3}{T}\right)\frac{e_4}{\theta_4 R_{N_2}} \times (e_3 + \theta_3 R_{CO_2}) - e_3\left(\frac{e_4}{\theta_4 R_{N_2}} + 1\right)\right] \quad (7)$$

$$\dot{w}_4 = [Z_{NN} P(\overset{10}{N},N) + Z_{NC} P(\overset{10}{N},C) + Z_{NH} P(\overset{10}{N},H)] \times \left[\exp\left(\frac{-\theta_4}{T}\right)\cdot(e_4 + \theta_4 R_{N_2}) - e_4\right] + Z_{NC} Q(\overset{01}{N},\underset{10}{C}3) + \left[(e_4 + \theta_4 R_{N_2})\frac{e_3}{\theta_3 R_{CO_2}} - \exp\left(\frac{\theta_4 - \theta_3}{T}\right)e_4\left(\frac{e_3}{\theta_3 R_{CO_2}} + 1\right)\right] \quad (8)$$

The preceding expressions for $\dot{w}_{12}, \dot{w}_3$, and $\dot{w}_4$ correspond to Eqs. (3.44-3.46) of Ref. 4, which should be consulted for the definition of terms and symbols. There is an error in Eq. (3.45) of Ref. 4 which is corrected in Eq. (6); the factor in Eq. (6) appears as 3 in Eq. (3.45) of Ref. 4, which is in error. This error appears to have originated in the older literature.[10]

Navier-Stokes Equations

The general two-dimensional conservation equations used in this analysis are

Continuity

$$\frac{\partial \rho}{\partial t} = -\left[\frac{\partial}{\partial x}(\rho u) + \frac{\partial}{\partial y}(\rho v)\right] \quad (9)$$

Species Continuity

$$\frac{\partial}{\partial t}(\rho c_i) = -\left[\frac{\partial}{\partial x}(\rho u c_i) + \frac{\partial}{\partial y}(\rho v c_i)\right] + \frac{\partial}{\partial x}\left(kD_{12}\frac{\partial c_i}{\partial x}\right) + \frac{\partial}{\partial y}\left(\rho D_{12}\frac{\partial c_i}{\partial y}\right) \quad (10)$$

x-Momentum

$$\frac{\partial}{\partial t}(\rho u) = -\left[\frac{\partial}{\partial x}(\rho uu) + \frac{\partial}{\partial y}(\rho vu)\right] - \frac{\partial p}{\partial x} + \frac{\partial}{\partial x}\left[2\mu\frac{\partial u}{\partial x} - \frac{2}{3}\mu\left(\frac{\partial u}{\partial x} + \frac{\partial v}{\partial y}\right)\right] + \frac{\partial}{\partial y}\left[\mu\left(\frac{\partial u}{\partial y} + \frac{\partial v}{\partial x}\right)\right] \quad (11)$$

y-Momentum

$$\frac{\partial}{\partial t}(\rho v) = -\left[\frac{\partial}{\partial x}(\rho uv) + \frac{\partial}{\partial y}(\rho vv)\right] - \frac{\partial p}{\partial y} + \frac{\partial}{\partial x} \times \left[\mu\left(\frac{\partial u}{\partial y} + \frac{\partial v}{\partial x}\right)\right] + \frac{\partial}{\partial y}\left[2\mu\frac{\partial v}{\partial y} - \frac{2}{3}\mu\left(\frac{\partial u}{\partial x} + \frac{\partial v}{\partial y}\right)\right] \quad (12)$$

Energy

$$\rho c_v \frac{\partial T}{\partial t} - RT\frac{\partial \rho}{\partial t} - \rho T\frac{\partial c_{N_2}}{\partial t}[R_{N_2} - R_2] = -[\rho u c_p \frac{\partial T}{\partial x} + \rho v c_p \frac{\partial T}{\partial y} + \rho_{CO_2}(\dot{w}_{12} + \dot{w}_3) + \rho_{N_2}\dot{w}_4] + \frac{\partial}{\partial x}\left(k\frac{\partial T}{\partial x}\right) + \frac{\partial}{\partial y}\left(k\frac{\partial T}{\partial y}\right) + u\frac{\partial p}{\partial x} + v\frac{\partial p}{\partial y} + \mu\Phi + \rho D_{12}\left[\frac{7}{2}\left(R_{N_2} - \frac{R_{CO_2}}{1+\alpha}\right) - \frac{\alpha}{1+\alpha}\left(\frac{\partial e^{eq}_{vib_{H_2O}}}{\partial T} + 4R_{H_2O}\right)\right]\cdot\left[\frac{\partial c_{N_2}}{\partial x}\frac{\partial T}{\partial x} + \frac{\partial c_{N_2}}{\partial y}\frac{\partial T}{\partial y}\right] \quad (13)$$

where

ρ_i = density of species i
ρ = static density
p = static pressure
T = static temperature
u = x component of velocity of the mixture
v = y component of velocity of the mixture
c_i = mass fraction of species i
μ = dynamic viscosity coefficient of the mixture
k = coefficient of thermal conductivity of the mixture
D_{12} = binary diffusion coefficient
$e^{eq}_{vib_{H_2O}}$ = equilibrium vibrational energy in H_2O
R_i = specific gas constant of species i
R = specific gas constant of the mixture

$$R = c_{N_2}R_{N_2} + c_{CO_2}R_{CO_2} + c_{H_2O}R_{H_2O}$$

$$R_2 = \frac{R_{CO_2}}{1+\alpha} + \frac{\alpha}{1+\alpha}R_{H_2O}$$

$$\alpha = \frac{c_{H_2O}}{c_{CO_2}}\ \text{(fixed)}$$

$$c_v = \frac{5}{2}R_{N_2}c_{N_2} + \frac{5}{2}R_{CO_2}c_{CO_2} + c_{H_2O}\left(3R_{H_2O} + \frac{\partial e^{eq}_{vib_{H_2O}}}{\partial T}\right)$$

$$c_p = c_v + R$$

$$\Phi = 2\left[\left(\frac{\partial u}{\partial x}\right)^2 + \left(\frac{\partial v}{\partial y}\right)^2\right] + \left(\frac{\partial v}{\partial x} + \frac{\partial u}{\partial y}\right)^2 - \frac{2}{3}\left(\frac{\partial u}{\partial x} + \frac{\partial v}{\partial y}\right)^2$$

Vibrational Relaxation Equations

$$\frac{\partial}{\partial t}(\rho e_{\text{vib}_{12}}) = -\frac{\partial}{\partial x}(\rho e_{\text{vib}_{12}} u) - \frac{\partial}{\partial y}(\rho e_{\text{vib}_{12}} v) + \frac{\partial}{\partial x}\left(\rho D_{12}\frac{\partial c_{\text{CO}_2}}{\partial x} e_{12}\right) + \frac{\partial}{\partial y}\left(\rho D_{12}\frac{\partial c_{\text{CO}_2}}{\partial y} e_{12}\right) + \rho_{\text{CO}_2}\dot{w}_{12} \tag{14}$$

$$\frac{\partial}{\partial t}(\rho e_{\text{vib}_3}) = -\frac{\partial}{\partial x}(\rho e_{\text{vib}_3} u) - \frac{\partial}{\partial y}(\rho e_{\text{vib}_2} v) + \frac{\partial}{\partial x}\left(\rho D_{12}\frac{c_{\text{CO}_2}}{\partial x} e_3\right) + \frac{\partial}{\partial y}\left(\rho D_{12}\frac{\partial c_{\text{CO}_2}}{\partial y} e_3\right) + \rho_{\text{CO}_2}\dot{w}_3 \tag{15}$$

$$\frac{\partial}{\partial t}(\rho e_{\text{vib}_4}) = -\frac{\partial}{\partial x}(\rho e_{\text{vib}_4} u) - \frac{\partial}{\partial y}(\rho e_{\text{vib}_4} v) + \frac{\partial}{\partial x}\left(\rho D_{12}\frac{\partial c_{\text{N}_2}}{\partial x} e_4\right) + \frac{\partial}{\partial y}\left(\rho D_{12}\frac{\partial c_{\text{N}_2}}{\partial y} e_4\right) + \rho_{\text{N}_2}\dot{w}_4 \tag{16}$$

where

$e_{12} = e(v_1) + 2e(v_2)$, $e_3 = e(v_3)$ } vibrational energy per unit mass of CO_2

$e_4 = e_{\text{vib}_{\text{N}_2}}$ = vibrational energy per unit mass of N_2

$e_{\text{vib}_{12}} = c_{\text{CO}_2} e_{12}$ = vibrational energy in mode 12 of CO_2 per unit mass of the mixture

$e_{\text{vib}_3} = c_{\text{CO}_2} e_3$ = vibrational energy in mode 3 of CO_2 per unit mass of the mixture

$e_{\text{vib}_4} = c_{\text{N}_2} e_4$ = vibrational energy in N_2 per unit mass of the mixture

The expressions for $\dot{w}_{12}, \dot{w}_3$, and $\dot{w}_4$ are given by Eqs. (6-8). The rate data obtained from Anderson[11] are used in the present study.

Mixture Properties

The gas mixture in the laser cavity consists of three gases, namely CO_2, N_2, and H_2O. CO_2 and N_2 are nonpolar gases and H_2O is a polar gas. However, the concentration of H_2O is negligibly small compared to N_2 and CO_2 concentrations. So, in calculating the transport properties, the mixture is treated as a binary mixture of CO_2 and N_2. This assumption simplifies the calculation of transport properties of a ternary mixture composed of polar and nonpolar gases.

The variation of viscosity coefficients and thermal conductivities of CO_2 and N_2 with temperature was obtained from Ref. 12. The viscosity of the mixture was calculated using Wilke's mixture role for gases at low pressure.[13] The thermal conductivity of the mixture was obtained using the Mason-Saxena formulation.[14] The binary diffusion coefficient D_{12} was calculated from standard kinetic theory.[15] For a more detailed description of the calculation of the mixture properties, the molecular properties and gas constants used in the present study, the reader is referred to Ref. 16.

III. Numerical Technique

The unsteady equations describing the flowfield variables are solved by means of an explicit, time-dependent, second-order accurate, finite-difference technique. The technique is patterned after the predictor-corrector approach of MacCormack,[17] with a modification of the finite differencing scheme.[18] The method has the advantage of being straightforward and inherently simple to program on a computer. Though many recent Navier-Stokes solutions have employed implicit techniques, no such scheme was implemented during the course of this investigation.

Let the flowfield illustrated in Fig. 1 be covered with a rectangular finite-difference mesh of grid points. At each grid point, initial values of all the flowfield variables ($p, T, u, v, e_{\text{vib}}$, etc.) are arbitrarily chosen. Let g denote one of these variables at a given grid point. Note that the left side of Eqs. (9-16) gives the first time derivatives of the flowfield quantities, whereas the right side contains only spatial derivatives in x and y. Using the known flowfield properties at time t, the first spatial derivatives are replaced by forward finite differences. The second spatial derivatives are computed as first derivatives of first derivatives by using a rearward finite-difference scheme. Thus, using a combination of forward and rearward differences, the time derivative $\partial g/\partial t$ is calculated. This allows "predicted" values of g, denoted by $\bar{g}$, to be obtained from

$$\bar{g}(t+\Delta t) = g(t) + \frac{\partial g}{\partial t}\Delta t$$

The values of $\bar{g}$ are then inserted into the right side of Eqs. (9-16). Using a combination of rearward and forward differences for the spatial derivatives, a "corrected" value of $\partial g/\partial t$, denoted by $\overline{\partial g/\partial t}$ is obtained. An average time derivative is calculated as the arithmetic mean of $\partial g/\partial t$ and $\overline{\partial g/\partial t}$. Then, the new value of g at a grid point is calculated from

$$g(t+\Delta t) = g(t) + \left(\frac{\partial g}{\partial t}\right)_{\text{ave}}\Delta t$$

This procedure is applied at all the grid points over many steps in time, and the value of g calculated at each time step is different. However, after a number of time steps, the differences become small, and g approaches a steady-state value. These steady-state values are the desired result. Various implications and improvisions on this scheme as applied to mixing flows are given in Ref. 19.

The time step Δt used above is chosen to satisfy the Courant-Friedrichs-Lewy (CFL) stability criterion.[20]

$$\Delta t \leq \text{minimum of}\left(\frac{\Delta x}{u+a}, \frac{\Delta y}{v+a}\right)$$

The CFL criterion was derived for a system of linear equations, and hence does not apply to the nonlinear flowfield equations. So the time step Δt is usually multiplied by a factor less than 1 (0.65 in the present investigation) to provide a stability criterion.

For systems with finite-rate processes, usually another criterion on Δt, dictated by the reaction rates also has to be considered.[21] The time step Δt should be smaller than the fastest rate for the system. In the present study, because of the low cavity pressures and the physical scales involved, the CFL time step turned out to be the smallest time step.

With regard to boundary conditions, examine Fig. 1. Let h be the distance between the centerlines of the two streams. The two nozzles shown are assumed to be only part of a bank of multiple nozzles characteristic of gasdynamic lasers, hence the two centerlines are lines of symmetry. Thus, at the boundary $y/h = 0$ and 1, standard symmetry conditions are imposed on velocities, mass-fractions, temperature, density, and vibrational energies. At these boundaries the gradients in the y direction vanish, except for v, which is set equal to zero. At the inlet to the laser cavity, $x/h = 0$, all conditions are given and held fixed with time. At the exit (generally taken as $x/h = 10$ for a given run) all properties are calculated by using one-sided rearward differences in both the predictor and

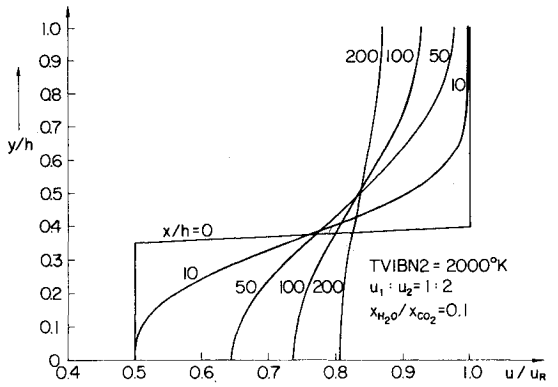

Fig. 3 Transverse profiles of velocity at various axial locations in the cavity.

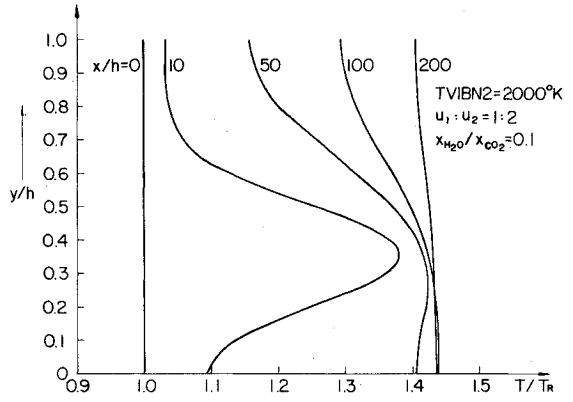

Fig. 4 Transverse profiles of static temperature at various axial locations in the cavity.

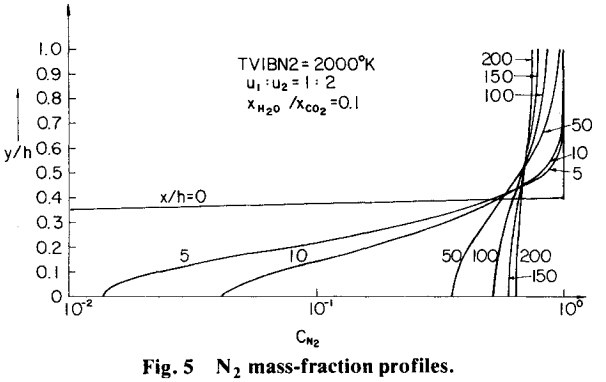

Fig. 5 N_2 mass-fraction profiles.

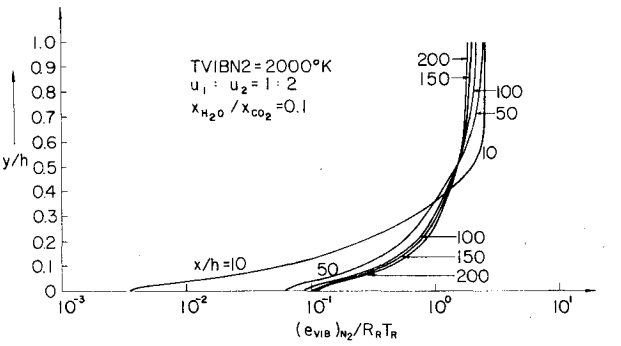

Fig. 6 Profiles of vibrational energy in N_2.

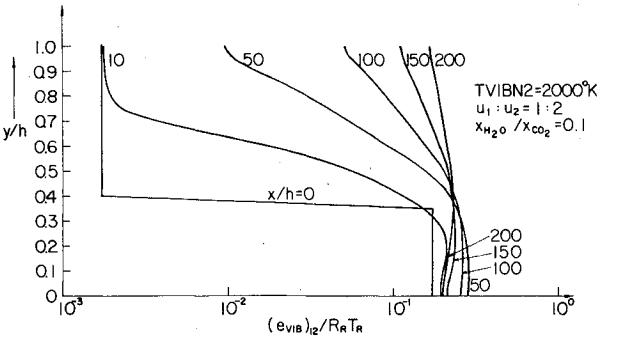

Fig. 7 Profiles of vibrational energy in mode 12.

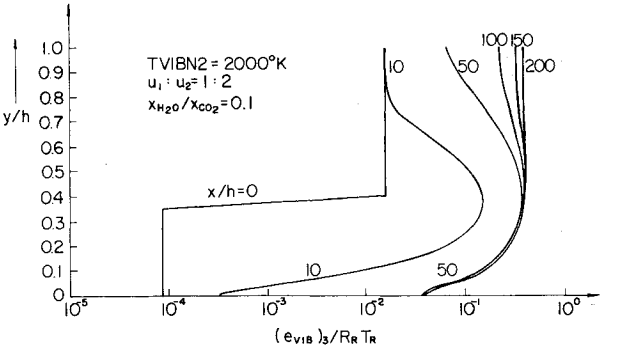

Fig. 8 Profiles of vibrational energy in mode 3.

corrector step of the finite-difference scheme. In order to calculate further downstream, a steady-state is first obtained for $0 \leq x/h \leq 10$. Then the steady-state results at $x/h = 10$ are assumed as fixed inlet conditions for a second time-dependent calculation from $x/h = 10$ to 20. This is repeated until the desired cavity length is calculated. In the present studies, flow results in a cavity of length $x/h = 200$ have been obtained in such a piecemeal fashion.

IV. Results and Discussion

Though the numerical method used to solve the flowfield equations is a time-dependent method, all results presented in this section are the final steady-state values. The intermediate transients are of no particular interest and are not given here.

The downstream mixing of two initially supersonic, vibrationally excited streams is a complex phenomenon. During the course of this investigation a stab was made at optimizing the small-signal gain in the laser cavity. It was found that the Reynolds number of the flow had to be kept small for reasons of numerical accuracy. This led to a study of laminar mixing. Further, it was not possible to hold all but one parameter of the problem fixed and carry out an optimization study. The following three studies were carried out. They were: 1) effect of velocity ratios between the two streams on gain, 2) effect of H_2O content on gain, and 3) effect of CO_2 on gain. The results of the optimization studies are also presented here. In the discussion of all the figures that follow, x_i is the mole-fraction of species i.

An explanation as to the reason for the choice of uniform profiles for velocity, temperature, and mass fractions at the exit of the nozzles is in order here. As stated earlier, for the low Reynolds numbers considered in the present study, thick boundary layers will be formed within the nozzles. The boundary-layer characteristics, such as thickness, velocity, temperature, and mass-fraction profiles depend strongly on the history of the flowfield inside the nozzle and on the shape and size of the nozzle. In order to keep the number of parameters that can be varied to a minimum, it was decided to use uniform profiles at the nozzle exits and thereby divorce the effect of the nozzle boundary layers on the small-signal gain optimization studies.

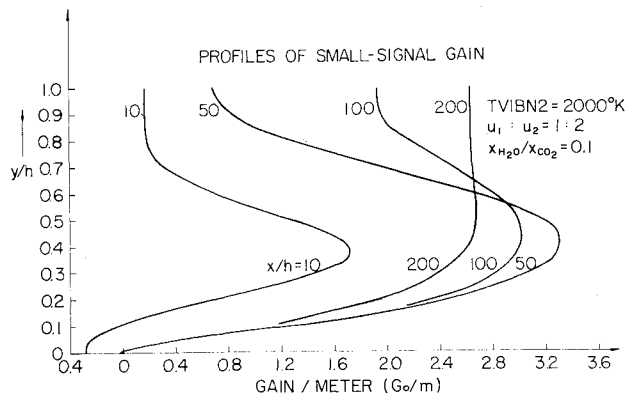

Fig. 9 Transverse profiles of G_0 at various axial locations in the cavity.

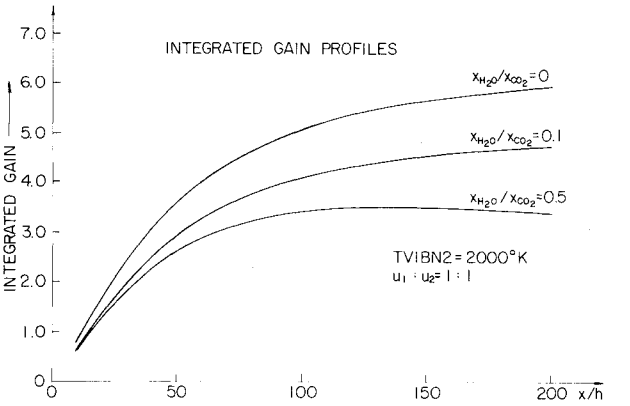

Fig. 11 Variation of integrated gain with distance along the flow; comparison between different H_2O contents.

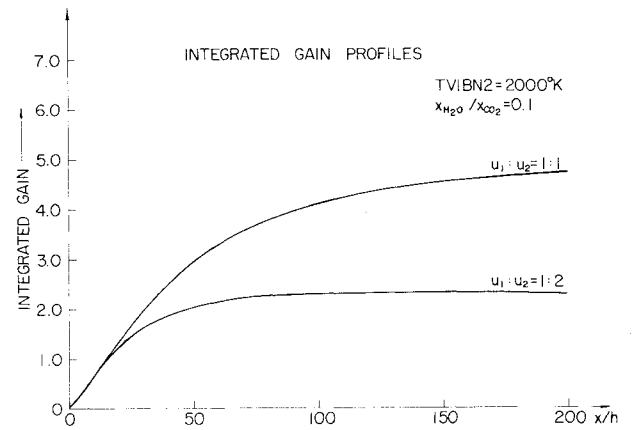

Fig. 10 Variation of integrated gain with distance along the flow; comparison between different velocity ratios. This is an "average" small-signal gain.

Consider Fig. 1, where the velocity ratio beteen the two streams is $u_1/u_2 = \frac{1}{2}$. The vibrational temperature of the N_2 stream is first assumed to be 2000 K. The conditions of the two streams at the inlet to the cavity are tabulated in Fig. 1. The resulting variation of the steady-state velocity profiles at various x/h locations along the cavity are shown in Fig. 3. Note that at $x/h = 200$, an almost uniform velocity is achieved across the complete flowfield. Such uniform flow conditions at $x/h = 200$ are further illustrated in Fig. 4, which shows the static temperature distributions across the flow at various x/h locations. Note that near the inlet, viscous dissipation within the mixing zone creates strong temperature gradients. These gradients become smaller as the flow progresses downstream; however, due to the combined effect of this viscous dissipation as well as collisional deactivation of vibrational energy to translational energy, the static temperature increases by almost 45% from the inlet to $x/h = 200$. Figure 5 is a plot of the N_2 mass-fraction profiles across the duct at various x/h locations in the laser cavity. The vibrational energy distributions in N_2 and in modes 12 and 3 of CO_2 are indicated in Figs. 6-8. The small-signal gain (G_0) profiles are shown in Fig. 9. Note the strong gradients in G_0 near the inlet; however, as the N_2 and CO_2-H_2O streams mix further downstream, a uniform gain region evolves, as shown by the upper portion of the curve at $x/h = 200$. It is clearly seen from Figs. 3-8 that for all practical purposes, the flow at $x/h = 200$ is very much like that of a conventional gasdynamic laser, except that the small-signal gain is at least a factor of 2 higher than a conventional GDL with the same reservior temperature of 2000 K. The profiles shown in Fig. 9 give the variation of G_0 in the y direction at selected x locations. If a given profile is integrated with respect to y/h, an integrated gain for the x location is obtained; such an integrated value is a representation of the overall laser quality of the mixing flow. The variation of this integrated gain as a function of x is shown as the lower curve in Fig. 10. Note that the integrated gain is virtually constant downstream of $x/h = 50$, a behavior beneficial to good laser quality. The upper curve in Fig. 10 is from a numerical experiment intended to assess the influence of velocity ratio; it gives the integrated gain when the CO_2-H_2O stream in Fig. 1 is at the same velocity (1878 m/s) as the N_2 stream, i.e., a one-to-one velocity ratio. In this case, the viscous dissipation is minimized, mixing is totally by diffusion, there is no meaningful increase in the static temperature due to mixing, and consequently the small-signal gain is higher because the population inversion is enhanced by low static temperatures. (At low T, the population of the 100 lower laser level in CO_2 is small, hence gain is increased; see Ref. 4 for details.)

Continuing with a one-to-one velocity ratio, Fig. 11 shows the influence of H_2O on the integrated gain. In the conventional GDL, small amounts of H_2O are necessary as a catalyst to insure reasonable depopulation of the lower laser level during the rapid nozzle expansion. However, in the case of a downstream-mixing GDL, the CO_2 stream is cool and in equilibrium as it enters the cavity, and the population of the lower laser level is already small. Hence, as shown in the diffusion-dominated case in Fig. 11, the best gain is obtained with no H_2O in the mixture. The water vapor only acts as a contaminant to degrade the laser performance for the conditions studied. The effect of H_2O on the gain is similar to that of H_2^{22} in that it interferes with the transfer of the reasonant, vibrational energy between N_2 and CO_2.

A word of caution is in order here regarding the effect of H_2O on downstream-mixing GDL's. When laser power is extracted in the cavity, the CO_2 molecules that are in the 001 level give out radiation and cascade down to either the 100 or 020 level in CO_2. In the absence of a catalyst, such as H_2O, to depopulate the lower laser level, the lower level gets clogged with CO_2 molecules, and the lasing action stops. So it is beneficial to have some H_2O for the operation of the laser with regard to power extraction.[23]

Figure 12 demonstrates the effect of increasing the vibrational temperature of the N_2 stream to 4000 K, and maintaining a one-to-one velocity ratio with no H_2O. Note that "average" integrated small-signal gains on the order of 11/m over a distance of $h = 6.82$ mm are obtained. This appears to be the highest small-signal gain yet reported for any detailed GDL calculations, and clearly demonstrates that the potential for downstream-mixing GDL's is promising even when the detailed collisional deactivation rate processes in the mixing zone are taken into account.

In order to assess the effect of CO_2 on small-signal gain, three different CO_2 nozzle sizes were used. In the case of the smallest CO_2 nozzle considered, five grid points were used to

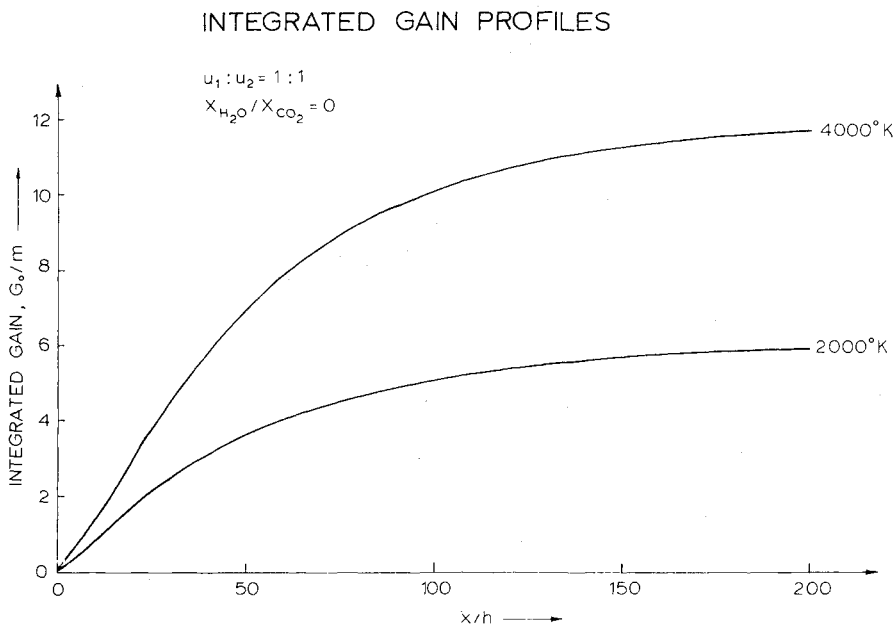

Fig. 12 Variation of integrated gain with distance along the flow; comparison between different N_2 vibrational temperatures.

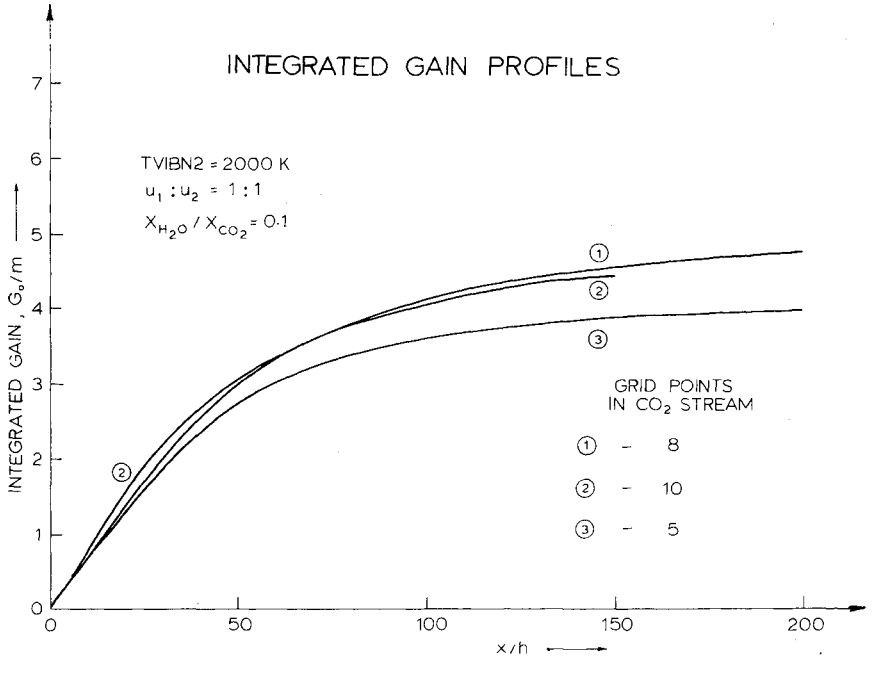

Fig. 13 Variation of integrated gain with distance along the flow; comparison between different CO_2 contents.

span the exit of the nozzle. Ten grid points were used for the largest nozzle. The results are graphically illustrated in Fig. 13. The small-signal gain was a maximum for a CO_2 nozzle of eight grid points. It should be mentioned here that all of the previous results that were given in Figs. 3-11 were for the CO_2 nozzle of eight grid points.

V. Conclusions

In light of the foregoing, the following conclusions can be made:

1) The downstream-mixing GDL is promising as a high-gain, high-energy laser concept, with substantial improvements over the conventional GDL. However, it must be noted that the thick boundary layers that originate within the small nozzles are not taken into account in the present calculations, and most likely will have a strong deleterious effect on laser performance. This aspect is now being studied. Also, note that the density nonhomogeneities in the mixing region will have an adverse effect on beam quality. This effect is outside the scope of the present work, which underscores the fluid dynamic and kinetic aspects of the mixing flow.

2) To minimize viscous heating of the mixing flow, the velocity ratio of the two streams should be one-to-one. For the low Reynolds number of such flows, mixing by laminar diffusion appears to be sufficient.

3) Though the small-signal gain is a maximum in the absence of water vapor, a small amount of water vapor is required for power extraction.

Acknowledgment

This work was supported by the Air Force Office of Scientific Research under AFOSR Grant No. 74-2575, and by the Minta Martin Fund for Aeronautical Research, an endowment given to the College of Engineering, University of Maryland, by the late Glenn L. Martin. Computer time was provided through the facilities of the Computer Science Center of the University of Maryland.

References

[1] Basov, N. G. and Oraevskii, A. N., "Attainment of Negative Temperatures by Heating and Cooling of a System," *Soviet Physics, JETP*, Vol. 17, Nov. 1963, pp. 1171-1172.

[2] Hurle, I. R. and Hertzberg, A., "Electronic Population Inversions by Fluid-Mechanical Techniques," *The Physics of Fluids*, Vol. 8, Sept. 1965, pp. 1601-1607.

[3] Gerry, E. T., "Gasdynamic Lasers," *IEEE Spectrum*, Vol. 7, Nov. 1970, pp. 51-58.

[4] Anderson, J. D., Jr., *Gasdynamic Lasers: An Introduction*, Academic Press, New York, 1976.

[5] Bronfin, B. R., Boedeker, L. R., and Cheyer, J. P., "Thermal Laser Excitation by Mixing in a Highly Convective Flow," *Applied Physics Letters*, Vol. 16, March 1970, pp. 214-217.

[6] Taran, J.P.E., Charpenel, M., and Borghi, R., "Investigation of a Mixing CO_2 GDL," AIAA Paper 73-622, Palm Springs, Calif., 1973.

[7] Croshko, V. N., Fomin, N. A., and Solukhin, R. I., "Population Inversion and Gain Distribution in Supersonic Mixed Flow Systems," *Acta Astronautica*, Vol. 2, Nov./Dec. 1975, pp. 929-939.

[8] Cassady, P., Newton, J., and Rose, P., "A New Mixing Gasdynamic Laser," *AIAA Journal*, Vol. 16, April 1978, pp. 305-312.

[9] Taylor, R. L. and Bitterman, S., "Survey of Vibrational Relaxation Data for Processes Important in the CO_2-N_2 Laser System," *Reviews of Modern Physics*, Vol. 41, Jan. 1969, pp. 26-47.

[10] Munjee, S. A., "Numerical Analysis of a Gasdynamic Laser Mixture," *The Physics of Fluids*, Vol. 15, March 1972, pp. 506-508.

[11] Anderson, J. D., Jr., "Effect of Kinetic Rate Uncertainties on Gasdynamic Laser Gain and Energy Predictions," *AIAA Journal*, Vol. 12, Dec. 1974, pp. 1699-1703.

[12] Svehla, R. A., "Estimated Viscosities and Thermal Conductivities of Gases at High Temperatures," NASA TR R-132, 1962.

[13] Wilke, C. R., "A Viscosity Equation for Gas Mixtures," *The Journal of Chemical Physics*, Vol. 18, April 1950, pp. 517-519.

[14] Mason, E. A. and Saxena, S. C., "Approximate Formula for the Thermal Conductivity of Gas Mixtures," *The Physics of Fluids*, Vol. 1, Sept.-Oct. 1958, pp. 361-369.

[15] Reid, R. C. and Sherwood, T. K., *The Properties of Gases and Liquids*, 2nd ed., McGraw-Hill, 1966, p. 523.

[16] Parthasarathy, K. N., Anderson, J.D., Jr., and Jones, E., "Downstream Mixing Gasdynamic Lasers—A Numerical Solution," AIAA Paper 79-0207, New Orleans, La., 1979.

[17] MacCormack, R. W., "The Effect of Viscosity in Hypervelocity Impact Cratering," AIAA Paper 69-354, Cincinnati, Ohio, 1969.

[18] Kothari, A. P. and Anderson, J. D., Jr., "Navier-Stokes Solutions for Chemical Laser Flows: Cold Flows," *AIAA Journal*, Vol. 14, May 1976, pp. 702-703.

[19] Jones, E. and Anderson, J. D., Jr., "Numerical Solutions of the Navier-Stokes Equations for Laminar and Turbulent Supersonic Mixing Flows," University of Maryland, College Park, Md., Aerospace Engineering Technical Rept., AE 75-5.

[20] Courant, R., Friedrichs, K. O., and Lewy, H., "Ueber die partiellen Differenzengleichungen der mathematischen Physik," *Mathematische Annalen*, Band 100, 1928, pp. 32-74.

[21] Anderson, J. D., Jr., "A Time-Dependent Analysis for Vibrational and Chemical Nonequilibrium Nozzle Flows," *AIAA Journal*, Vol. 8, March 1970, pp. 545-550.

[22] Hoffman, R., Juegell, H., and Schall, W., "Contaminants in a Gasdynamic Mixing Laser," *AIAA Journal*, Vol. 15, Oct. 1977, pp. 1527-1529.

[23] Cassady, P., Private communication, Mathematical Sciences Northwest, Inc., Bellevue, Wash.